Thermal Radiation Effects on Mhd Free Convection Flow of a Micropolar Fluid Past a Stretching Surface Embedded in a Non-Darcian Porous Medium

S Mohammed Ibrahim[1]   T Sankar Reddy[2]   and N Bhaskar Reddy[3]

[1] Department of Mathematics, Priyadarshini College of Enggineering and Technology, Nellore – 524004, A. P., India .

[2] Deparment of Mathematics, Annamacharyya College of Engineering and Technology, Cuddapa, A . P., India.

[3] Department of Mathematics, Sri Venkateswara University, Tirupathi – 517502, A. P. India.

Email: ibrahimsvu@gmail.com.

ABSTRACT

A comprehensive study of thermal radiation on a steady two-dimensional laminar flow of a viscous incompressible electrically conducting micropolar fluid past a stretching surface embedded in a non-Darcian porous medium is analyzed numerically. The governing equations of momentum, angular momentum, and energy equations are solved numerically using Runge- Kutta fourth order method with shooting technique. The effects of various parameters on the velocity, microrotation, and temperature field as well as skin friction coefficient, and Nusselt number are shown graphically and in tabulated. It is observed that the micropolar fluid helps in the reduction of drag forces and also acts as a cooling agent.

KEYWORDS: Micropolar fluid, Free convection, Darcy number,Radiation, MHD, Porous medium.

1. INTRODUCTION

Micropolar fluids are fluid with microstructure. They belong to a class of fluids with nonsymmetric stress tensor that we shall call polar fluids. Micropolar fluids may also represent fluids consisting of rigid, randomly oriented (or spherical) particles suspended in a viscous medium, where the deformation of the particle is ignored. This constitutes a substantial generalization of the Navier-Stokes model and opens a new field of potential applications. The attractiveness and power of the model of micropolar fluids come from the fact that it is both a significant and a simple generalization of the classical Navier-Stokes model. The theory of micropolar fluids developed by Eringen [1] and has been a field of very active research for the last few decades as this class of fluids represents, mathematically, many industrial important fluids such as paints, body fluids, polymers, colloidal fluids, suspension fluids, animal blood, liquid crystal, etc among the various non-Newtonian fluids model. Eringen[2] has also developed the theory of thermomicropolar fluids by the extending the theory of micropolar fluids. A thorough review of the subject of the application of micropolar fluid mechanics has been given by Lukaszewicz [3] and Arimanm et al [4]. Ahmadi [5] obtained a similarity solution for micropolar boundary layer flow over a semi-infinite plate. Jena and Mathur [6] further studied the laminar free convection flow of thermomicropolar fluids past a non-isothermal vertical plate.

Boundary-layer flow and heat transfer over a continuously stretched surface has received considerable attention in recent years. This stems from various possible engineering and metallurgical applications such as a hot rolling, wire drawing. Metal and plastic extrusion, continuous casting, glass fiber production, crystal growing, and paper production. The continuous surface concept was introduced by sakiadis [7,8]. Rajagopal et al [9] studied a boundary layer flow a non-Newtonian over a stretching sheet with a uniform free stream. Hady [10] studied the solution of a heat transfer to a micropolar fluid from a non- isothermal stretching sheet with injection. Na and Pop [11] investigated the boundary layer flow of micropolar fluid due to a stretching wall. Hassanien et al [12] studied a numerical solution for heat transfer in a micropolar fluid over a stretching sheet. Desseaux and Kelson [13] studied the flow of micropolar fluid bounded by stretching sheet. In all the above studies, the authors have taken the stretching sheet to be an oriented in horizontal direction. However, of late the effects of MHD to the micropolar fluids problem are very important. Abo – Eldahab and Ghonaim [14] investigated the convective heat transfer in an electrically conducting micropolar fluid at a stretching surface with uniform free stream. Pavlov [15] studied the boundary layer flow of an electrically conducting fluid due to a stretching of a plane elastic surface in the presence of a uniform transverse magnetic field. Chakrabarti and Gupta [16] extended Pavlov's work to study the heat transfer when a uniform suction is applied at the stretching surface.

Many processes in engineering areas occur at high temperatures and knowledge of radiating heat transfer becomes very important for the design of the pertinent equipment. Nuclear power plants, gas turbines and the various propulsion devices for aircraft, missiles, satellites and space vehicles are examples of such engineering areas. Abo-Eldahad and Ghonaim [17] analyzes the radiation effects on heat transfer of a micropolar fluids through a porous medium. Ishak [18] studied the thermal boundary layer flow over a stretching sheet in a micropolar fluid with radiation. Gnaneswar [19] studied the heat generation and thermal radiation effects over a stretching sheet in a micropolar fluid. Olanrewaju et al. [20] found radiation effects on MHD flow of micropolar fluid towards a stagnation point on a vertical plate.

However the interaction of radiation effect of an electrically conducting micropolar fluid past a stretching surface has received little attention. Hence an attempt is made to investigate the radiation effects on a steady free convection flow near an isothermal vertical stretching sheet in the presence of a magnetic field, a non-Darcian porous medium. The governing equations are transformed by using similarity transformation and the resultant dimensionless equations are solved numerically using the Runge-Kutta fourth order method with shooting technique. The effects of various governing parameters on the velocity temperature, skin-friction coefficient and Nusselt number are shown in figures and tables and analyzed in detail.
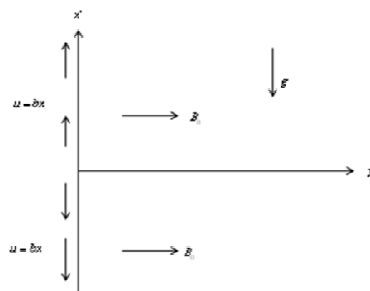
MATHEMATICAL FORMULATION

Fig. 1. Sketch of the physical model.

Let us consider a steady, two-dimensional laminar, free convection boundary layer flow of an electrically conducting and heat generating/absorbing micropolar fluid through a porous medium bounded by a vertical iso-thermal sheet coinciding with the plane y = 0, where the flow confined to y > 0. Two equal and opposite forces are introduced along the x' - axis so that the sheet is linearly stretched keeping the origin fixed (see Fig.1). A uniformly distributed transverse magnetic field of strength B_0 is imposed along the y' – axis. The magnetic Reynolds number of the flow is taken to be small enough so that the induced distortion of the applied magnetic field can be neglected. The viscous dissipative heat is also assumed to be negligible. It is also assumed that microscopic inertia term involving J (where J is the square of the characteristic length of microstructure) can be neglected for steady two – dimensional boundary layer flow in a micropolar fluid without introducing any appreciable error in the solution. Under the above assumptions and upon treating the fluid saturated porous medium as continuum, including the non-Darcian inertia effects, and assuming that the Boussinesq approximation is valid, the boundary layer form of the governing equations can be written as (Willson [21] ,Nield and Bejan [22])

$$\frac{\partial u'}{\partial x'} + \frac{\partial v'}{\partial y'} = 0$$

(1)

$$u'\frac{\partial u'}{\partial x'} + v'\frac{\partial v'}{\partial y'} = v\frac{\partial^2 u'}{\partial y'^2} + g\beta(T' - T'_\infty) + k_1\frac{\partial \sigma'}{\partial y'} - \frac{\sigma_0 B_0^2}{\rho}u' - \frac{v}{K}u' - Cu'^2$$

(2)

$$G_1\frac{\partial^2 \sigma}{\partial y'^2} - 2\sigma - \frac{\partial u'}{\partial y'} = 0$$

(3)

$$u'\frac{\partial T'}{\partial x'} + v'\frac{\partial T'}{\partial y'} = \frac{k_e}{\rho c_p}\frac{\partial^2 T'}{\partial y'^2} - \frac{1}{\rho c_p}\frac{\partial q_r}{\partial y'}$$

(4)

Subject to the boundary conditions:

$$u' = bx, \quad v' = 0, \quad T' = T'_w, \quad \sigma = 0 \quad \text{at } y = 0,$$

$$u' \to u'_\infty, T' \to T'_\infty, \sigma = 0 \text{ as } y \to \infty$$

(5)

where x' and y' are the coordinates along and normal to the sheet. u' and v' are the components of the velocity in the x' and y'- directions, respectively. σ, k_1 and G_1 are the microrotation component, coupling constant, and microrotation constant, respectively. k_e, C, K, T' are the effective thermal conductivity, permeability of the porous medium, transport property related to the inertia effect, fluid temperature respectively. $\beta,, U_\infty$ and g are the coefficient of thermal expansion, coefficient of concentration expansion, volumetric rate of heat generation, free stream velocity, and acceleration due to gravity, respectively. σ_0, ρ, v and c_p are the electrical conductivity, density, apparent kinematic viscosity, and specific heat at constant pressure of the fluid, respectively.

By using the Rosseland approximation (Brewster [23]), the radiative heat flux in y' direction is given by

$$q_r = -\frac{4\sigma^*}{3k^*}\frac{\partial T'^4}{\partial y'}$$

(6)

where σ^* is the Stefan-Boltzmann constant and k^* is the mean absorption coefficient. By using (7) , the energy equation (4) becomes

$$u'\frac{\partial T'}{\partial x'} + v'\frac{\partial T'}{\partial y'} = \frac{k_e}{\rho c_p}\frac{\partial^2 T'}{\partial y'^2} + \frac{4\sigma^*}{3k^*\rho c_p}\frac{\partial^2 T'^4}{\partial y'^2}$$

(7)

It is convenient to make the governing equations and conditions dimensionless by using

$$x = \frac{bx'}{u'_\infty} \qquad y = \frac{by'}{u'_\infty}R \qquad u = \frac{u'}{u'_\infty} \qquad v = \frac{v'}{u'_\infty}R \qquad R = \frac{u_\infty}{\sqrt{cv}} \qquad \theta = \frac{T' - T''_\infty}{T'_w - T'_\infty}$$

$$M = \frac{\sigma_0 B_0^2}{\rho b} \quad Gr = \frac{g\beta(T'_w - T'_\infty)}{bu'_\infty}$$

(8)

$$\mathrm{Pr} = \frac{\mu c_p}{k} \qquad F = \frac{kk^*}{4\sigma^* T_\infty^3} \qquad r = \frac{T'_w - T'_\infty}{T'_\infty}$$

$$\gamma = \frac{Cu_\infty}{b} \qquad \sigma = \frac{v\sigma'}{u_\infty^2} R \qquad Da^{-1} = \frac{v}{Kb}$$

In view of the equation (8), the equations (1), (2), (3) and (8) reduce to the following non-dimensional form.

$$\frac{\partial u}{\partial x} + \frac{\partial v}{\partial y} = 0 \tag{9}$$

$$u\frac{\partial u}{\partial x} + v\frac{\partial u}{\partial y} = \frac{\partial^2 u}{\partial y^2} + N_1\frac{\partial \sigma}{\partial y} - Mu - \frac{1}{Da}u - \gamma u^2 + Gr\theta \tag{10}$$

$$G\frac{\partial^2 \sigma}{\partial y^2} - 2\sigma - \frac{\partial u}{\partial y} = 0 \tag{11}$$

$$u\frac{\partial \theta}{\partial x} + v\frac{\partial \theta}{\partial y} = \frac{1}{\mathrm{Pr}}\frac{\partial^2 \theta}{\partial y^2} + \frac{4}{3F\mathrm{Pr}}\left((1+r\theta)^3\frac{\partial^2 \theta}{\partial y^2} + 3r(1+r\theta)^2\left(\frac{\partial \theta}{\partial y}\right)^2\right) \tag{12}$$

The corresponding boundary conditions are

$$u = x \qquad v = 0 \qquad \sigma = 0 \qquad \theta = 1 \qquad \text{at} \quad y = 0,$$

$$u = 1 \quad \sigma = 0 \quad \theta = 0 \quad \text{as} \qquad y \to \infty \tag{13}$$

where R is the Reynolds number. Proceeding with the analysis, we define a stream function $\psi(x, y)$ such that

$$u = \frac{\partial \psi}{\partial \overline{y}}, v = -\frac{\partial \psi}{\partial \overline{x}} \tag{14}$$

Now, let us consider the stream function as if

$$\psi(x, y) = f(y) + xg(y)$$
(15)

$$\sigma = xh(y)$$
(16)

In view of equation (14) – (16), the continuity equation (9) is identically satisfied and the momentum equation (10), angular momentum equation (11), energy equation (12) becomes

$$\frac{\partial \psi}{\partial y}\frac{\partial^2 \psi}{\partial x\partial y} - \frac{\partial \psi}{\partial x}\frac{\partial^2 \psi}{\partial y^2} = \frac{\partial^3 \psi}{\partial y^3} + \left(M + \frac{1}{Da}\right)\frac{\partial \psi}{\partial y} + \gamma\left(\frac{\partial \psi}{\partial y}\right)^2 - Gr\theta \tag{17}$$

$$\frac{\partial \psi}{\partial y}\frac{\partial \theta}{\partial x} - \frac{\partial \psi}{\partial x}\frac{\partial \theta}{\partial y} = \frac{1}{\mathrm{Pr}}\frac{\partial^2 \theta}{\partial y^2} + \frac{4}{3F\mathrm{Pr}}\left((1+r\theta)^3\frac{\partial^2 \theta}{\partial y^2} + 3r(1+r\theta)^2\left(\frac{\partial \theta}{\partial y}\right)^2\right) \tag{18}$$

$$G\frac{\partial^2 \sigma}{\partial y^2} - 2\sigma - \frac{\partial u}{\partial y} = 0 \tag{19}$$

and the boundary conditions (13) become

$$\frac{\partial \psi}{\partial y} = x \qquad \frac{\partial \psi}{\partial x} = 0 \qquad h = 0 \qquad \theta = 1 \qquad at \ y = 0$$

$$\frac{\partial \psi}{\partial y} \to 1 \ h \to 0 \ \theta \to 0 \text{ as } y \to \infty \tag{20}$$

in equations (17), (18),(19) and equating coefficient of x^0 and x^1, we obtain the coupled non-linear ordinary differential equations

$$f''' + f''g - f'g' - \left(M + \frac{1}{Da}\right)f' - \gamma f'^2 + Gr\theta = 0 \tag{21}$$

$$g''' + gg'' - (g')^2 - \left(M + \frac{1}{Da}\right)g' - 2\gamma f'g' + N1h' = 0$$
(22)

$$Gh'' - 2h - g'' = 0$$
(23)

$$\left(3F + 4(1 + r\theta)^3\right)\theta'' + 3\Pr Fg\theta' + 12r(1 + r\theta)^2 \theta'^2 = 0 \tag{24}$$

where a prime denotes differentiation with respect to y.

In view of (17) and (18) , the boundary conditions (23) reduce to

$$f = 0 \qquad f' = 0 \qquad g = 0 \qquad g' = 1 \qquad h = 1 \qquad \theta = 1 \qquad at \quad y = 0$$

$$f' \to 1 \quad g' \to 0 \quad h \to 0 \quad \theta \to 0 \qquad as \quad y \to \infty \tag{25}$$

Of special significance in free convection problems are the skin-friction coefficient, Neusselt number

The shear stress at the stretching surface is given by

$$\tau_w = (\mu + k)\left(\frac{\partial u'}{\partial y'}\right)_{y'=0} + k(\sigma)_{y'=0} = \rho vbR\left(\frac{\partial u}{\partial y}\right)_{y=0}$$

$$= \rho vbR\left[f''(0) + xg''(0)\right]. \tag{26}$$

The skin-friction coefficient C_f is given by

$$C_f = \frac{\tau_w}{\frac{1}{2}\rho u_\infty^2} = \frac{2}{R}\left[f''(0) + xg''(0)\right]. \tag{27}$$

The wall heat flux is given by

$$q_w = -k\left(\frac{\partial T'}{\partial y'}\right)_{y'=0} = -k\frac{bR}{u_\infty}\left(\frac{\partial T'}{\partial y'}\right)_{y'=0} = -k\frac{bR}{u_\infty}(T'_w - T'_\infty)\theta'(0).$$

(28)

Nussel number $\quad Nu = \dfrac{q_w}{k(T'_w - T'_\infty)} = \dfrac{bR}{u_\infty}\theta'(0)$.   (29)

NUMERICAL PROCEDURE

The shooting method for linear equations is based on replacing the boundary value problem by two initial value problems and the solutions of the boundary value problem is a linear combination between the solutions of the two initial value problems. The shooting method for the non-linear boundary value problem is similar to the linear case, except that the solution of the non-linear problem cannot be simply expressed as a linear combination of the solutions of the two initial value problems. Instead, we need to use a sequence of suitable initial values for the derivatives such that the tolerance at the end point of the range is very small. This sequence of initial values is given by the secant method, and we use the fourth order Runge-Kutta method to solve the initial value problems.

Following Rosenhead [24] and Carnahan et al [25], the value of y at infinity is fixed at 5. The full equations (21) - (24) with the boundary conditions (25) were solved numerically using Runge-Kutta method algorithm with a systematic guessing $f''(0), g''(0), h'(0), \theta'(0)$ by the shooting technique until the boundary conditions at infinity $f'(y)$ decay exponentially to one, also $g'(y), h(y), \theta(y)$ to zero. The functions $f', g', -h \;\; \theta$ are shown in Figures.

RESULTS AND DISCUSSION

As a result of the numerical calculations, the dimensionless velocity, angular velocity , temperature and concentration distributions for the flow under consideration are obtained and their behavior have been discussed for variations in the governing parameters viz., the thermal Grashof number Gr, solutal Grashof number Gc, magnetic field parameter M, Radiation parameter F, the parameter of relative difference between the temperature of the sheet and temperature far away from the sheet r, Prandtl number Pr, Darcy number, porous medium inertia coefficient γ, vortes viscosity parameter $N1$, microrotation parameter G. In the present study, the following default parametric values are adopted. $Gr = 0.5$, $Gc = 0.5$, $M = 0.01$, $Pr = 0.71$, $F = 1.0$, $r = 0.05$, $\gamma = 0.01$, $N1 = 0.1$, $G = 2.0$, $Da = 100$. All graphs therefore correspond to these unless specifically indicated on the appropriate graph.

Fig.1(a). Shows the variation of the dimensionless velocity component f' for several sets of values of thermal Grashof number Gr. As expected, it is observed that there is a rise in the velocity due to enhancement of thermal buoyancy force.

The effect of variation of the magnetic parameter M on the velocity $\;\;(\; f'$ and $\;g'$), angular velocity – h, temperature θ and concentration ϕ profiles is presented in Figs. 2(a) – 2(d) respectively. It is will know that the application of a uniform magnetic field normal to the flow direction gives rise to a force called Lorentz. This force has the tendency to slow down the velocity of the fluid and angular velocity of microrotation in the boundary layer and to increase its temperature. This is obvious from the decreases in the velocity profiles, angular velocity of microrotation profiles, while temperature profiles increases, presented in Figs. 2(a) – 2(d) respectively.

Figs. 3(a) – 3(d) present typical profiles for the variables of the fluid's x – component of velocity (f' and $\;g'$), angular velocity –h, temperature θ for different values of Darcy number Da. It is noted that values of Da increases the fluid velocities and angular velocity increases, while temperature of the fluid be decreases.

Figs. 4(a) – 4(d) present the typical profiles for the variables of the fluid's x – component of velocity (f' and g'), angular velocity $-h$, temperature θ for different values of the porous medium inertia coefficient γ. Obviously, the porous medium inertia effects constitute resistance to the flow. Thus as the inertia coefficient increases, the resistance to the flow increases, causing the fluid flow in the porous medium to slow down and the temperature, concentration increases and, therefore, as γ increases f', g' and $-h$ decreases while the temperature θ

Figs. 5(a) – 5(d) present the typical profiles for the variables of the fluid's x – component of velocity (f' and g'), angular velocity $-h$, temperature θ for different values of the vortex viscosity parameter $N1$. Increase in the values of $N1$ have a tendency to increase $f', -h, \theta$ and to decrease g'.

Fig. 6 is a plot of the dimensionless angular velocity $-h$ profiles for different values of the presence of the microrotation parameter G. The curves illustrate that, as the values of G increases, the angular velocity $-h$, as expected, decreases with an increase in the boundary layer thickness as the maximum moves away from the sheet. Of course, when the viscosity of the fluid decreases the angular velocity of additive increase.

Fig.7(a). Illustrates the dimensionless velocity component f' for different values of the Prandtl number Pr. The numerical results show that the effect of increasing values of Prandtl number results in a decreasing velocity. From fig.7(b), it is observed that an increase in the Prandtl number results a decrease of the thermal boundary layer thickness and in general lower average temperature within the boundary layer.
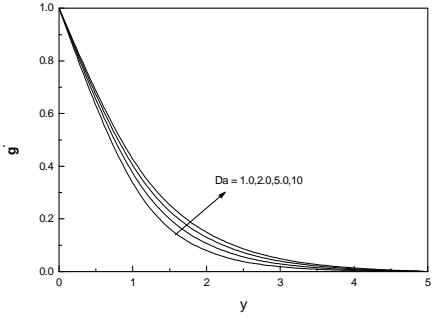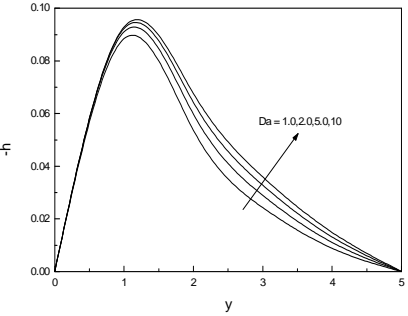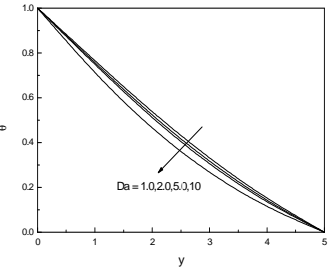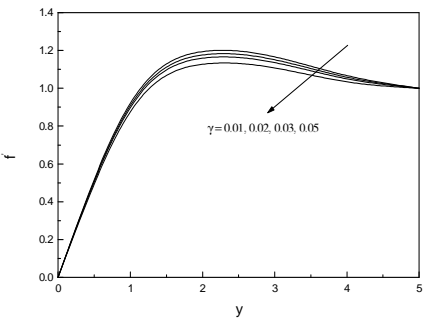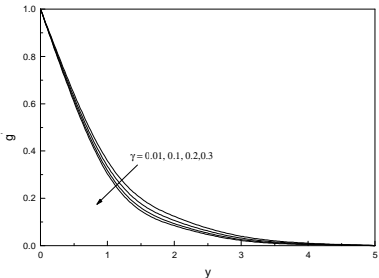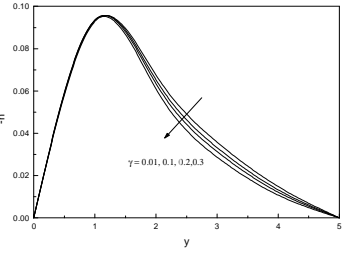
The effect of the Radiation parameter F on the dimensionless velocity component f' and dimensionless temperature are shown in Figs. 8(a) and 8(b) respectively. Fig.8 (a) shows that velocity component f' decreases with an increase in the radiation parameter F. From Fig.8(b) it is seen that the temperature decreases as the radiation parameter F increases. This result qualitatively agrees with expectations, since the effect of radiation is to decrease the rate of energy transport to the fluid, thereby decreasing the temperature of the fluid.
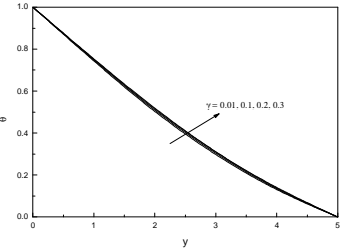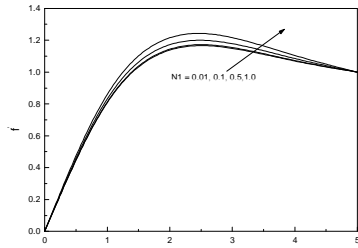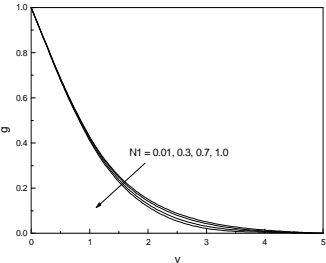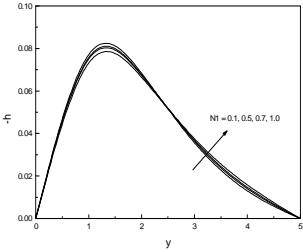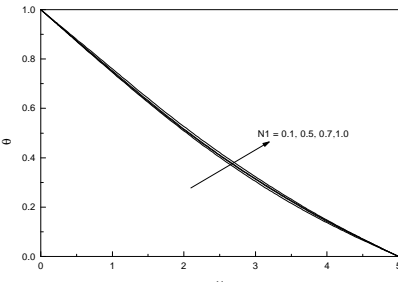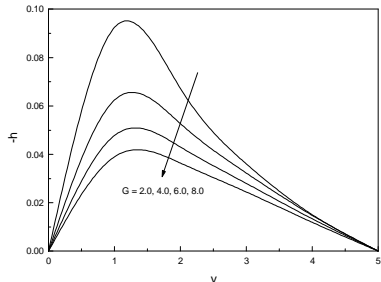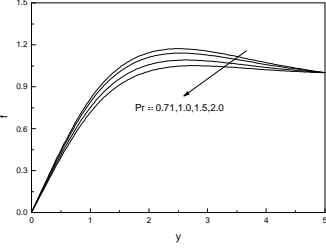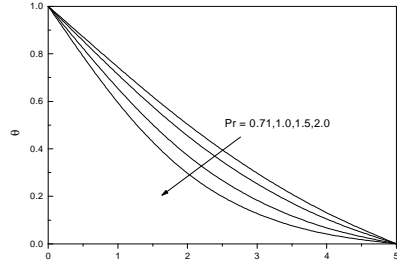
The influence of the parameter of relative difference between the temperature of the sheet and the temperature far away from the sheet r on dimensionless velocity f' and temperature profiles are plotted in Figs. 9(a) and 9(b) respectively. Fig.9(a) shows that dimensionless velocity f' increases with an increase in r. It is observed that the temperature increases with an increase in r (Fig.9 (b)).

Table 1 illustrates the missing wall functions for velocity, angular velocity, temperature and concentration functions. These quantities are useful in evaluation of wall shear stresses, gradient of angular velocity, surface heat transfer rate and mass transfer rate. The results are obtained for $r = 0.05$ and different values of the the thermal Grashof number Gr, magnetic field parameter M, Radiation parameter F, the parameter of relative difference between the temperature of the sheet and temperature far away from the sheet r, Prandtl number Pr, Darcy number Da , porous medium inertia coefficient γ , vortes viscosity parameter $N1$, microrotation parameter G . From Table 1 indicate that increasing the values of the Grashof number Gr result in an increase in the values of $f''(0)$. This is because as Gr increase, the momentum boundary layer thickness decreases and, therefore, an increase in the values of $f''(0)$ occurs. The results indicate that a distinct fall in the skin-frction coefficient in the x – direction ($f''(0)$ and $g''(0)$),the surface heat transfer rate $-\theta'(0)$, while gradient of angular velocity $h'(0)$ increases , accompanies a rise in the magnetic field parameter M. Increases in the values of Da has the effect of increasing the skin-friction function $f''(0)$, heat transfer rate $-\theta'(0)$ while gradient of angular velocity $h'(0)$, the skin-friction function $g''(0)$ slightly decreases as Da increases. Further, the influence of the porous medium inertia coefficient γ on the wall shear stresses, gradient of angular velocity, surface heat transfer is the same as that of the inverse Darcy number Da^{-1} since it also represents resistance to the flow. Namely, as γ increases, $f''(0), \theta'(0)$, decrease while $g''(0), -h'(0)$ slightly increases, respectively.

From Table 2 that for given values of *Gr, M, Da*, γ, an increase in the values of microrotation parameter *N1* leads to reduction in the skin-friction function $g''(0), \theta'(0)$ while the skin-friction function $f''(0)$, gradient of angular velocity $h'(0)$, increase as *N1* increases. The skin friction $f''(0)$ increase and the gradient of angular velocity $h'(0)$ is decreased as the microrotation parameter *G* increases, while the skin-friction coefficient in the *x*- directions $g''(0)$ heat transfer rate $-\theta'(0)$ are insensible to change in *G*. Increasing the values of heat generation parameter λ result in an increase in values of $f''(0)$ and the heat transfer rate $-\theta'(0)$ decrease. It is observed that the magnitude of the wall temperature gradient increases as Prandtl number *Pr* or radiation parameter *F* increases. Furthermore, the negative values of the wall temperature and concentration gradients, for all values of the dimensionless parameters, are indicative of the physical fact that the heat flows from the sheet surface to the ambient fluid.

Fig.1 variation of the velocity component f' with *Gr*

Fig.2(a) variation of the velocity component f' with *M*

Fig.2(b) variation of the velocity component g' with *M*

Fig.2(c) variation of the velocity component $-h$ with *M*

Fig.2(d) variation of the velocity component θ with *M*

Fig.3(a) variation of the velocity component f'
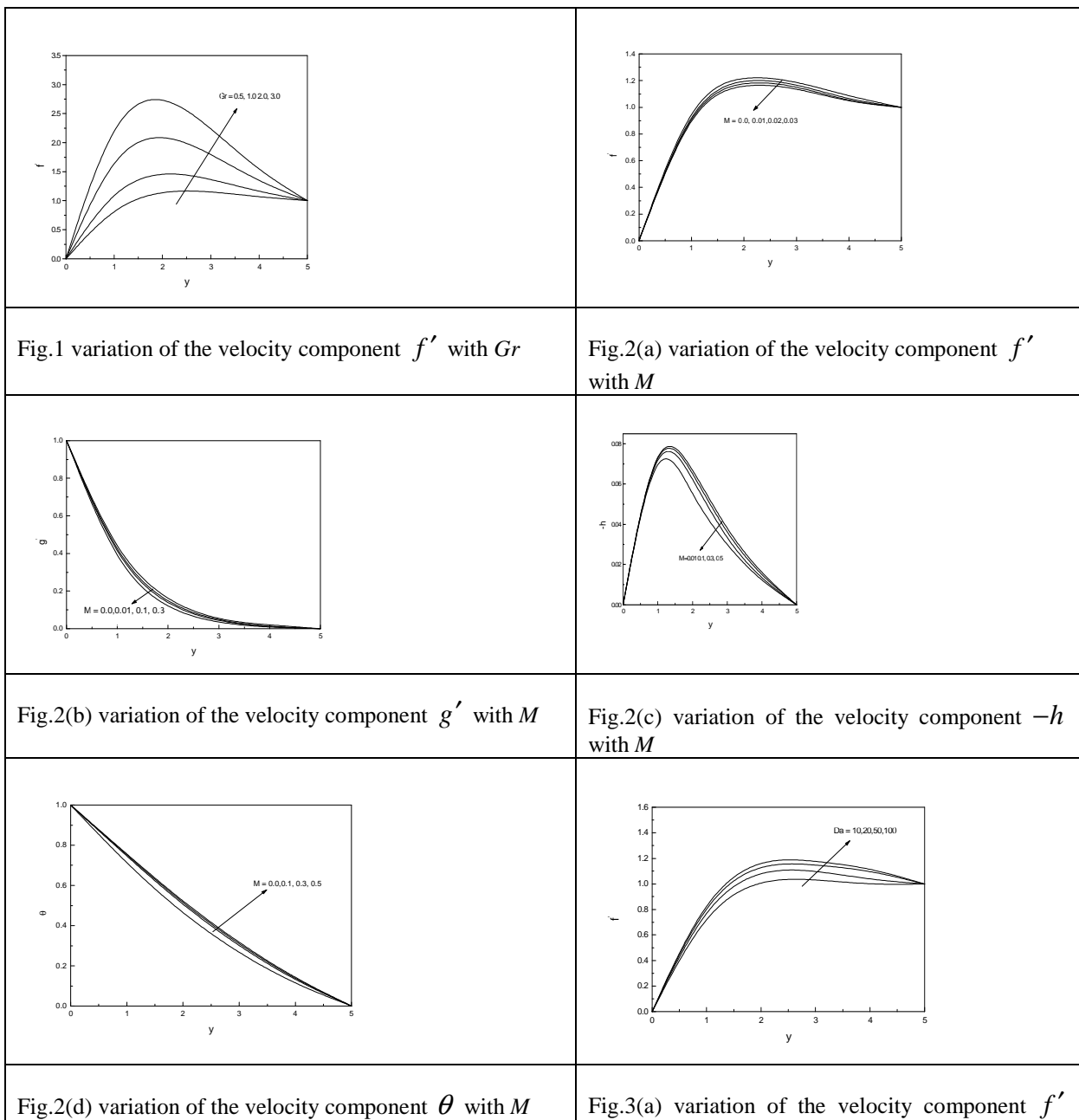
with Da	
Fig.3(b) variation of the velocity component g' with Da	Fig.3(c) variation of the velocity component $-h$ with Da
Fig.3(d) variation of the velocity component θ with Da	Fig.4(a) variation of the velocity component f' with γ
Fig.4(b)variation of the velocity component g' with γ	Fig.4(c) variation of the velocity component $-h$ with γ

|	
Fig.4(d) variation of the velocity component θ with γ	Fig.5(a) variation of the velocity component f' with $N1$
Fig.5(b)variation of the velocity component g' with $N1$	Fig.5(c)variation of the velocity component $-h$ with $N1$
Fig.5(d)variation of the velocity component θ	Fig.6 variation of the velocity component $-h$ with G
Fig.7(a) variation of the velocity component f' with Pr	Fig.7(b) variation of the velocity component θ with Pr

Fig.8(a) variation of the velocity component f' with F

Fig.8(b) variation of the velocity component θ with F

Fig.9(a) variation of the velocity component f' with r

Fig9(b) variation of the velocity component θ with r
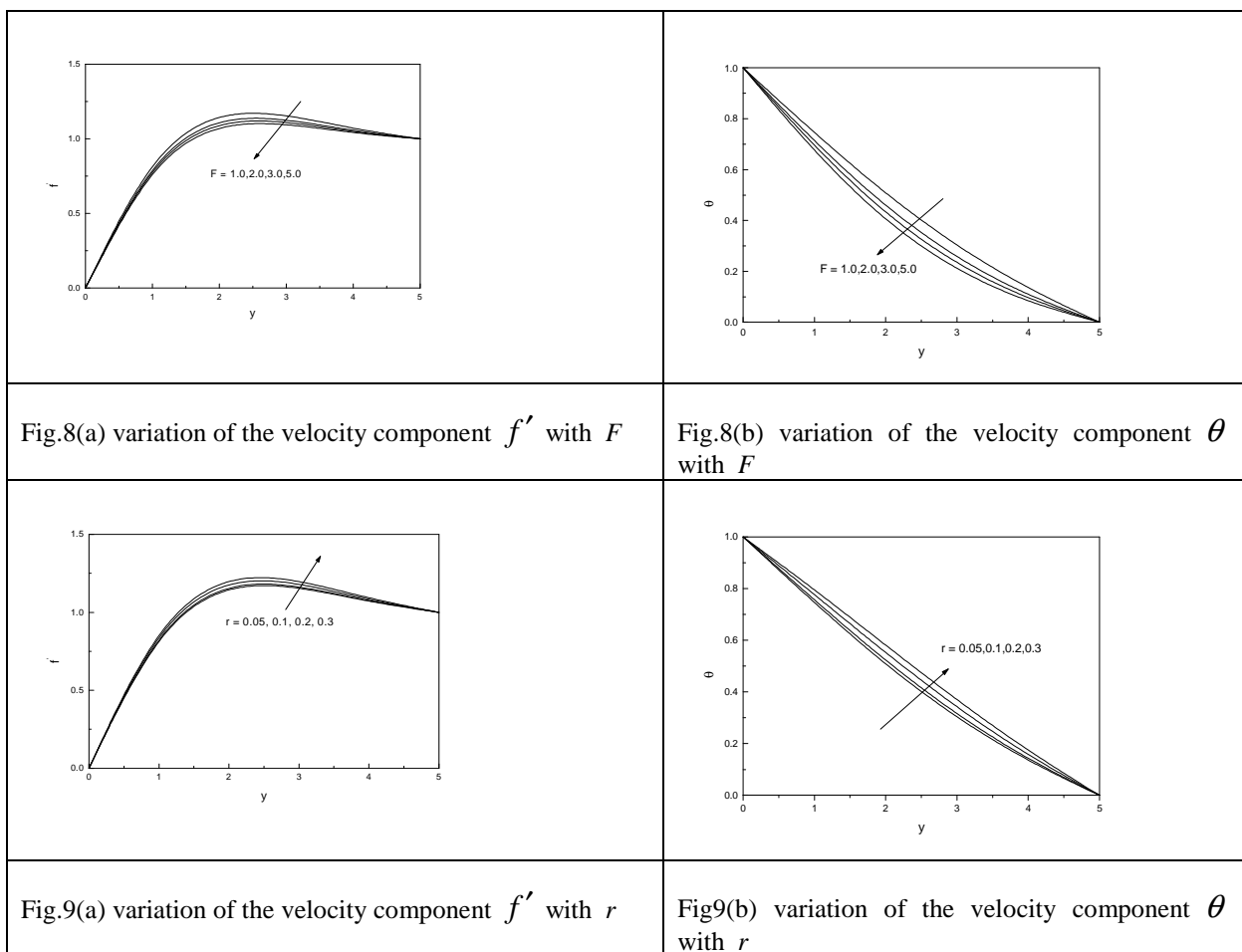
Table 1 Variation of $f'', g'', -h', \theta', \phi'$ at the plate with *Gr, M, Da* and γ for *Pr = 0.71, F = 1.0, r = 0.05.*

Gr	M	Da	γ	$f''(0)$	$g''(0)$	$h'(0)$	$-\theta'(0)$
0.5	0.1	100	0.01	1.21865	-1.05339	0.25808	0.27721
1.0	0.1	100	0.01	1.72256	-1.05339	0.25833	0.276989
0.5	0.2	100	0.01	1.64847	-1.05339	0.25827	0.277042
0.5	0.1	10	0.01	1.11425	-1.05275	0.26313	0.272843
0.5	0.1	20	0.01	1.12368	-1.09429	0.26264	0.273265
0.5	0.1	100	0.1	1.17407	-1.09973	0.26014	0.275425

Table 3 Variation of $f'', g'', -h', \theta'$ at the plate with *G, Pr, N1, F* for *Gr = 0.5, M = 0.1, Da = 100.*

G	Pr	N1	F	$f''(0)$	$g''(0)$	$-h'(0)$	$\theta'(0)$
2	0.71	0.1	1.0	1.12865	-1.05339	0.25808	0.27721
4	0.71	0.1	1.0	1.21747	-1.05339	0.15006	0.27721
2	1.0	0.1	1.0	1.1752	-1.05339	0.25805	0.33548
2	0.71	0.4	1.0	1.22994	-1.03823	0.25937	0.27557

CONCLUSIONS

The problem of steady, laminar, free convection boundary layer flow of micropolar fluid from a vertical stretching surface embedded in a non –Darcian porous medium in the presence of thermal radiation, uniform magnetic field and free stream velocity was investigated. A similarity transformation was employed to change the governing partial differential equations into ordinary one. These equations were solved numerically by fourth order Rung – Kutta along with Shooting technique. A wide selection of numerical results have been presented giving the evolution of the velocity, microrotation, temperature profiles as well as the skin- friction coefficient, heat transfer rate. It was found that the skin-friction coefficient, heat transfer rate are decreased and gradient of angular velocity increases as the inverse Darcy number, porous medium inertia coefficient, or magnetic field parameter is increased. It was noticed that in increase in radiation parameter or Prandtl number caused decrease in the skin-friction coefficient and increase in heat transfer rate.

REFERENCES

1. Eringen AC (1966), Theory of micropolar fluids, Journal of Mathematics and Mechanics. Vol. 16, pp. 1-18.
2. Eringen AC (1972), Theory of thermomicrofluids, Journal of Mathematical Analysis and Applications. Vol. 38, pp. 480-496.
3. Lukaszewicz G (1999), Micropolar fluids-theory and applications. Birkhauser, Boston.
4. Arimann T, Turk MA, and Sylvester ND (1973), Microcontinuum fluid Mechanics --- A Review, Int. J of Engg. Sci. Vol. 11,pp.905-930.
5. Ahamadi G (1976), Self-similar solution of incompressible micropolar boundary layer flow over a semi-infinite plate. Int. J. of Engg.Sci. Vol.14(7),pp.639-646.
6. Jena SK and Mathur MN (1981), Similarity solutions for laminar free convection flow of a thermomicropolar fluid past a non-isothermal vertical flat plate, Int J. of Engg Sci. Vol.19(11),pp.1431-1439.
7. Sakiadis BC (1961) Boundary-layer on continuous solid surface. Am. Inst.Chem.Eng. J, Vol 7,pp.26-28.
8. Sakiadis BC (1961) Boundary-layer behavior on continuous moving solid surface. Am. Inst.Chem.Eng. J, Vol 7,pp.221-225.
9. RajaGopal KR, Na TY and Gupta AS (1987), A non-similar boundary layer on a stretching sheet in a non-Newtonian fluid with uniform free stream, J. Maths Phys Sci Vol(2),pp.189-200.
10. Hady FM (1996), Short communication on the solution of heat transfer to micropolar fluid from a non-isothermal stretching sheet with injection. Int J Num Meth. Heat Fluid Flow, Vol.6,pp.99-104.
11. Na TY and Pop I (1997), Boundary layer flow of micropolar fluid due to stretching wall, Arch.Appl.Mech, Vol.67,pp.229-234.
12. Hassanien I, Gorla RSR, and Abdulah AA (1998), Numerical solution for heat transfer in micropolar fluids over a stretching sheet, Appl.Mech.Engg, Vol.3,pp.3-12.
13. Desseaux A and Kelson NA (2000), Flow of micropolar fluid bounded by stretching sheet, ANZIAM J, Vol.42,pp.532-560.
14. Abo-Eldahab EM and Ghonaim AF (2003), Convective heat transfer in an electrically conducting micropolar fluid at a stretching surface with uniform free stream, Appl.Math.Comp,Vol.137(2),pp.323-336.

15. Pavlov KB (1974), Magnetohydrodynamic flow of an incompressible viscous fluid caused by deformation of a surface.Magn.Gidrodin, Vol.4,pp.146-147.

16. Chakrabarti A and Gupta AS (1979) Hydromagnetic flow and heat transfer over a stretching sheet, Quart.Appl.Math,Vol.33,pp.73-78.

17. Khedr MEM, Chamkha AJ and Bayomi M (2009), MHD flow of a micropolar fluid past a stretched permeable surface with heat generation or absorption. Nonlinear Analysis.Modelling and Control, Vol.14(1),pp.27-40.

18. Abo-Eldahad EM and Ghonaim AF (2005), Radiation effect on heat transfer of a micropolar fluid through a porous medium, App. Mathematics and Computation, Vol.169(1),pp.500-516.

19. Gnaneswara Reddy M (2012), Heat generation and thermal radiation effects over a stretching sheet in a micropolar fluid. ISRN Thermodynamics. Vol.6.pp.1-6.

20. Olanrewaju PO, Okedayo GT and Gbadeyan JA (2011), Effects of thermal radiation on magnetohydrodynamic flow of a micropolar fluid towards a stagnation point on a vertical plate, International Journal of Applied Science and Technology, Vol.1,pp.1-6.

21. Willson AJ (1970), Boundary layer in micropolar liquids, Mathematical Proceeding of the Cambridge Philosophical Society, Vol.67(2),pp.469-476.

22. Nield DA and Bejan A (1999), convection in porous media, Springer, Newyork.

23. Brewster MQ (1992), Thermal radiative Transfer and properties, John Wiley and Sons, New York.

24. Rosenhead L (1963), Laminar Boundary, Oxford University Press, Oxford.

25. Carnahan B, Luther HA and James OW (1969), Applied Numerical Methods, Wiley, New York.